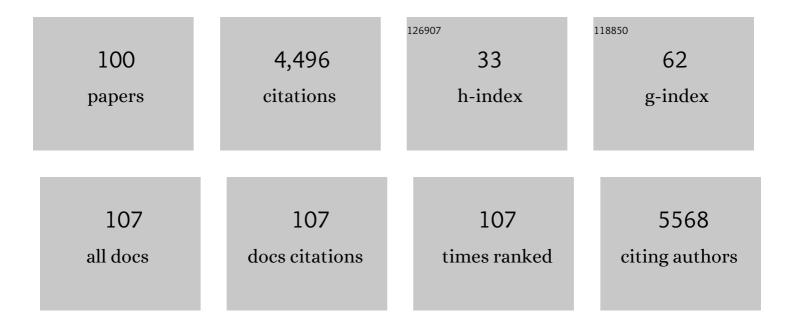
List of Publications by Year in descending order

Source: https://exaly.com/author-pdf/9468466/publications.pdf Version: 2024-02-01



DÃYI STENMADE

#	Article	IF	CITATIONS
1	MTH1 inhibition eradicates cancer by preventing sanitation of the dNTP pool. Nature, 2014, 508, 215-221.	27.8	419
2	The ALFA-tag is a highly versatile tool for nanobody-based bioscience applications. Nature Communications, 2019, 10, 4403.	12.8	278
3	Identification and characterization of a novel botulinum neurotoxin. Nature Communications, 2017, 8, 14130.	12.8	196
4	The Crystal Structure of the Human Toll-like Receptor 10 Cytoplasmic Domain Reveals a Putative Signaling Dimer. Journal of Biological Chemistry, 2008, 283, 11861-11865.	3.4	171
5	Small-molecule inhibitor of OGG1 suppresses proinflammatory gene expression and inflammation. Science, 2018, 362, 834-839.	12.6	156
6	Crystal Structure of Botulinum Neurotoxin Type A in Complex with the Cell Surface Co-Receptor GT1b—Insight into the Toxin–Neuron Interaction. PLoS Pathogens, 2008, 4, e1000129.	4.7	150
7	The Radical Site in Chlamydial Ribonucleotide Reductase Defines a New R2 Subclass. Science, 2004, 305, 245-248.	12.6	143
8	Botulinum and Tetanus Neurotoxins. Annual Review of Biochemistry, 2019, 88, 811-837.	11.1	140
9	MEMBRANE-BOUNDDIIRONCARBOXYLATEPROTEINS. Annual Review of Plant Biology, 2003, 54, 497-517.	18.7	134
10	Identification of a Botulinum Neurotoxin-like Toxin in a Commensal Strain of Enterococcus faecium. Cell Host and Microbe, 2018, 23, 169-176.e6.	11.0	127
11	A comprehensive structural, biochemical and biological profiling of the human NUDIX hydrolase family. Nature Communications, 2017, 8, 1541.	12.8	124
12	A New Member of the Family of Di-iron Carboxylate Proteins. Journal of Biological Chemistry, 2001, 276, 33297-33300.	3.4	118
13	Crystal structure, biochemical and cellular activities demonstrate separate functions of MTH1 and MTH2. Nature Communications, 2015, 6, 7871.	12.8	96
14	NUDT15 Hydrolyzes 6-Thio-DeoxyGTP to Mediate the Anticancer Efficacy of 6-Thioguanine. Cancer Research, 2016, 76, 5501-5511.	0.9	96
15	Massively parallel variant characterization identifies <i>NUDT15</i> alleles associated with thiopurine toxicity. Proceedings of the National Academy of Sciences of the United States of America, 2020, 117, 5394-5401.	7.1	95
16	Botulinum neurotoxin D-C uses synaptotagmin I/II as receptors and human synaptotagmin II is not an effective receptor for type B, D-C, and G toxins. Journal of Cell Science, 2012, 125, 3233-42.	2.0	90
17	EPR Studies of the Mitochondrial Alternative Oxidase. Journal of Biological Chemistry, 2002, 277, 43608-43614.	3.4	75
18	Crystal structure of human MTH1 and the 8-oxo-dGMP product complex. FEBS Letters, 2011, 585, 2617-2621.	2.8	70

#	Article	IF	CITATIONS
19	Crystal Structure of the Emerging Cancer Target MTHFD2 in Complex with a Substrate-Based Inhibitor. Cancer Research, 2017, 77, 937-948.	0.9	67
20	Structure of dual receptor binding to botulinum neurotoxin B. Nature Communications, 2013, 4, 2058.	12.8	65
21	The structure of human collapsin response mediator protein 2, a regulator of axonal growth. Journal of Neurochemistry, 2007, 101, 906-917.	3.9	63
22	The structure of the tetanus toxin reveals <scp>pH</scp> â€mediated domain dynamics. EMBO Reports, 2017, 18, 1306-1317.	4.5	61
23	Crystal Structure of Human Cytosolic 5′-Nucleotidase II. Journal of Biological Chemistry, 2007, 282, 17828-17836.	3.4	56
24	Targeted NUDT5 inhibitors block hormone signaling in breast cancer cells. Nature Communications, 2018, 9, 250.	12.8	56
25	A prokaryotic alternative oxidase present in the bacteriumNovosphingobium aromaticivorans. FEBS Letters, 2003, 552, 189-192.	2.8	55
26	Organellar oligopeptidase (OOP) provides a complementary pathway for targeting peptide degradation in mitochondria and chloroplasts. Proceedings of the National Academy of Sciences of the United States of America, 2013, 110, E3761-9.	7.1	50
27	Glycans Confer Specificity to the Recognition of Ganglioside Receptors by Botulinum Neurotoxin A. Journal of the American Chemical Society, 2017, 139, 218-230.	13.7	50
28	A neurotoxin that specifically targets Anopheles mosquitoes. Nature Communications, 2019, 10, 2869.	12.8	50
29	Crystal Structure of Human Inosine Triphosphatase. Journal of Biological Chemistry, 2007, 282, 3182-3187.	3.4	48
30	Engineered botulinum neurotoxin B with improved efficacy for targeting human receptors. Nature Communications, 2017, 8, 53.	12.8	46
31	Discovery of the First Potent and Selective Inhibitors of Human dCTP Pyrophosphatase 1. Journal of Medicinal Chemistry, 2016, 59, 1140-1148.	6.4	40
32	Hypoxic Signaling and the Cellular Redox Tumor Environment Determine Sensitivity to MTH1 Inhibition. Cancer Research, 2016, 76, 2366-2375.	0.9	40
33	Structure of the native pyruvate dehydrogenase complex reveals the mechanism of substrate insertion. Nature Communications, 2021, 12, 5277.	12.8	39
34	Crystal Structure of the Botulinum Neurotoxin Type G Binding Domain: Insight into Cell Surface Binding. Journal of Molecular Biology, 2010, 397, 1287-1297.	4.2	36
35	Cofactor mobility determines reaction outcome in the IMPDH and GMPR (β-α)8 barrel enzymes. Nature Chemical Biology, 2011, 7, 950-958.	8.0	35
36	Purification, Modeling, and Analysis of Botulinum Neurotoxin Subtype A5 (BoNT/A5) from Clostridium botulinum Strain A661222. Applied and Environmental Microbiology, 2011, 77, 4217-4222.	3.1	34

#	Article	IF	CITATIONS
37	Structural basis of inhibition of the human serine hydroxymethyltransferase <scp>SHMT</scp> 2 by antifolate drugs. FEBS Letters, 2019, 593, 1863-1873.	2.8	34
38	Structure of the synthetase domain of human CTP synthetase, a target for anticancer therapy. Acta Crystallographica Section F: Structural Biology Communications, 2006, 62, 613-617.	0.7	33
39	Fragment-Based Discovery and Optimization of Enzyme Inhibitors by Docking of Commercial Chemical Space. Journal of Medicinal Chemistry, 2017, 60, 8160-8169.	6.4	32
40	The Manganese Ion of the Heterodinuclear Mn/Fe Cofactor in <i>Chlamydia trachomatis</i> Ribonucleotide Reductase R2c Is Located at Metal Position 1. Journal of the American Chemical Society, 2012, 134, 123-125.	13.7	30
41	Crystal Structures of Botulinum Neurotoxin DC in Complex with Its Protein Receptors Synaptotagmin I and II. Structure, 2013, 21, 1602-1611.	3.3	30
42	Structural characterisation of the catalytic domain of botulinum neurotoxin X - high activity and unique substrate specificity. Scientific Reports, 2018, 8, 4518.	3.3	30
43	Pharmacological targeting of MTHFD2 suppresses acute myeloid leukemia by inducing thymidine depletion and replication stress. Nature Cancer, 2022, 3, 156-172.	13.2	30
44	Mechanism of Peptide Binding and Cleavage by the Human Mitochondrial Peptidase Neurolysin. Journal of Molecular Biology, 2018, 430, 348-362.	4.2	29
45	Engineered botulinum neurotoxin B with improved binding to human receptors has enhanced efficacy in preclinical models. Science Advances, 2019, 5, eaau7196.	10.3	29
46	Targeting OGG1 arrests cancer cell proliferation by inducing replication stress. Nucleic Acids Research, 2020, 48, 12234-12251.	14.5	29
47	Crystal Structure of CaiB, a Type-III CoA Transferase in Carnitine Metabolismâ€. Biochemistry, 2004, 43, 13996-14003.	2.5	28
48	Structural studies of tri-functional human GART. Nucleic Acids Research, 2010, 38, 7308-7319.	14.5	28
49	The Crystal Structure of the Bifunctional Deaminase/Reductase RibD of the Riboflavin Biosynthetic Pathway in Escherichia coli: Implications for the Reductive Mechanism. Journal of Molecular Biology, 2007, 373, 48-64.	4.2	27
50	Structural basis for the unique ganglioside and cell membrane recognition mechanism of botulinum neurotoxin DC. Nature Communications, 2017, 8, 1637.	12.8	26
51	Cotranslational Folding of a Pentarepeat β-Helix Protein. Journal of Molecular Biology, 2018, 430, 5196-5206.	4.2	25
52	The Structure and Classification of Botulinum Toxins. Handbook of Experimental Pharmacology, 2019, 263, 11-33.	1.8	25
53	Vinylic MIDA Boronates: New Building Blocks for the Synthesis of Azaâ€Heterocycles. Chemistry - A European Journal, 2015, 21, 7394-7398.	3.3	23
54	Small-molecule activation of OGG1 increases oxidative DNA damage repair by gaining a new function. Science, 2022, 376, 1471-1476.	12.6	20

#	Article	IF	CITATIONS
55	DNA compaction by the bacteriophage protein Cox studied on the single DNA molecule level using nanofluidic channels. Nucleic Acids Research, 2016, 44, gkw352.	14.5	19
56	The structure of the PP2A regulatory subunit B56 ^{î3} : The remaining piece of the PP2A jigsaw puzzle. Proteins: Structure, Function and Bioinformatics, 2009, 74, 212-221.	2.6	18
57	Characterization of a membrane binding loop leads to engineering botulinum neurotoxin B with improved therapeutic efficacy. PLoS Biology, 2020, 18, e3000618.	5.6	18
58	The Crystal Structure of a Human PP2A Phosphatase Activator Reveals a Novel Fold and Highly Conserved Cleft Implicated in Protein-Protein Interactions. Journal of Biological Chemistry, 2006, 281, 22434-22438.	3.4	17
59	Structure of the high-valent FellIFelV state in ribonucleotide reductase (RNR) of Chlamydia trachomatis—Combined EPR, 57Fe-, 1H-ENDOR and X-ray studies. Biochimica Et Biophysica Acta - Proteins and Proteomics, 2007, 1774, 1254-1263.	2.3	14
60	Crystal structures of OrfX2 and P47 from a Botulinum neurotoxin OrfXâ€ŧype gene cluster. FEBS Letters, 2017, 591, 3781-3792.	2.8	14
61	Crystal Structure of Botulinum Neurotoxin A2 in Complex with the Human Protein Receptor SV2C Reveals Plasticity in Receptor Binding. Toxins, 2018, 10, 153.	3.4	14
62	Development of a chemical probe against NUDT15. Nature Chemical Biology, 2020, 16, 1120-1128.	8.0	14
63	Crystal structures of human PAICS reveal substrate and product binding of an emerging cancer target. Journal of Biological Chemistry, 2020, 295, 11656-11668.	3.4	14
64	MutT homologue 1 (MTH1) catalyzes the hydrolysis of mutagenic O6-methyl-dGTP. Nucleic Acids Research, 2018, 46, 10888-10904.	14.5	13
65	Structure and steroid isomerase activity of <i>Drosophila</i> glutathione transferase E14 essential for ecdysteroid biosynthesis. FEBS Letters, 2020, 594, 1187-1195.	2.8	13
66	A ribonucleotide reductase from Clostridium botulinum reveals distinct evolutionary pathways to regulation via the overall activity site. Journal of Biological Chemistry, 2020, 295, 15576-15587.	3.4	12
67	Screening for functional expression and overexpression of a family of diiron-containing interfacial membrane proteins using the univector recombination system. Protein Science, 2003, 12, 124-134.	7.6	11
68	A comparison of X-ray and calculated structures of the enzyme MTH1. Journal of Molecular Modeling, 2016, 22, 168.	1.8	11
69	Human NUDT22 Is a UDP-Glucose/Galactose Hydrolase Exhibiting a Unique Structural Fold. Structure, 2018, 26, 295-303.e6.	3.3	11
70	Crystal Structures and Inhibitor Interactions of Mouse and Dog MTH1 Reveal Species-Specific Differences in Affinity. Biochemistry, 2018, 57, 593-603.	2.5	11
71	NUDT15 polymorphism influences the metabolism and therapeutic effects of acyclovir and ganciclovir. Nature Communications, 2021, 12, 4181.	12.8	11
72	Structures of the hydrolase domain of human 10-formyltetrahydrofolate dehydrogenase and its complex with a substrate analogue. Acta Crystallographica Section D: Biological Crystallography, 2006, 62, 1294-1299.	2.5	10

#	Article	IF	CITATIONS
73	The crystal structure of human cleavage and polyadenylation specific factorâ€5 reveals a dimeric Nudix protein with a conserved catalytic site. Proteins: Structure, Function and Bioinformatics, 2008, 73, 1047-1052.	2.6	10
74	Crystal structure of the P2 C-repressor: a binder of non-palindromic direct DNA repeats. Nucleic Acids Research, 2010, 38, 7778-7790.	14.5	10
75	Germline variation in the oxidative DNA repair genes NUDT1 and OGG1 is not associated with hereditary colorectal cancer or polyposis. Human Mutation, 2018, 39, 1214-1225.	2.5	10
76	MutT homologue 1 (MTH1) removes N6-methyl-dATP from the dNTP pool. Journal of Biological Chemistry, 2020, 295, 4761-4772.	3.4	10
77	Structural insight into DNA binding and oligomerization of the multifunctional Cox protein of bacteriophage P2. Nucleic Acids Research, 2014, 42, 2725-2735.	14.5	9
78	NUDT15-mediated hydrolysis limits the efficacy of anti-HCMV drug ganciclovir. Cell Chemical Biology, 2021, 28, 1693-1702.e6.	5.2	9
79	Structural and functional studies of the human phosphoribosyltransferase domain containing protein 1. FEBS Journal, 2010, 277, 4920-4930.	4.7	8
80	Crystal structure of the catalytic domain of the <i>Weissella oryzae</i> botulinumâ€like toxin. FEBS Letters, 2019, 593, 1403-1410.	2.8	8
81	Crystal structures of NUDT15 variants enabled by a potent inhibitor reveal the structural basis for thiopurine sensitivity. Journal of Biological Chemistry, 2021, 296, 100568.	3.4	8
82	Crystal Structure and Substrate Specificity of the 8-oxo-dGTP Hydrolase NUDT1 from <i>Arabidopsis thaliana</i> . Biochemistry, 2019, 58, 887-899.	2.5	7
83	Structural basis for the interaction of the chaperone Cbp3 with newly synthesized cytochrome b during mitochondrial respiratory chain assembly. Journal of Biological Chemistry, 2019, 294, 16663-16671.	3.4	6
84	Structural and Biochemical Characterization of Botulinum Neurotoxin Subtype B2 Binding to Its Receptors. Toxins, 2020, 12, 603.	3.4	6
85	Structural and Biochemical Investigation of Class I Ribonucleotide Reductase from the Hyperthermophile <i>Aquifex aeolicus</i> . Biochemistry, 2022, 61, 92-106.	2.5	6
86	The First Structure of Human MTHFD2L and Its Implications for the Development of Isoform elective Inhibitors. ChemMedChem, 2022, 17, .	3.2	6
87	GRETA, a new multifermenter system for structural genomics and process optimization. Acta Crystallographica Section D: Biological Crystallography, 2006, 62, 1227-1231.	2.5	5
88	Mechanism of Ganglioside Receptor Recognition by Botulinum Neurotoxin Serotype E. International Journal of Molecular Sciences, 2021, 22, 8315.	4.1	5
89	Structural Analysis of Botulinum Neurotoxins Type B and E by Cryo-EM. Toxins, 2022, 14, 14.	3.4	5
90	Crystals of the ribonucleotide reductase R2 protein fromChlamydia trachomatisobtained by heavy-atom co-crystallization. Acta Crystallographica Section D: Biological Crystallography, 2004, 60, 376-378.	2.5	4

#	Article	IF	CITATIONS
91	Novel spirocyclic systems via multicomponent aza-Diels–Alder reaction. Organic and Biomolecular Chemistry, 2017, 15, 7758-7764.	2.8	4
92	Structural and functional analysis of the inhibition of equine glutathione transferase A3-3 by organotin endocrine disrupting pollutants. Environmental Pollution, 2021, 268, 115960.	7.5	4
93	Crystal structure of the bacteriophage P2 integrase catalytic domain. FEBS Letters, 2015, 589, 3556-3563.	2.8	3
94	Nudix hydrolase 18 catalyzes the hydrolysis of active triphosphate metabolites of the antivirals remdesivir, ribavirin, and molnupiravir. Journal of Biological Chemistry, 2022, 298, 102169.	3.4	3
95	Synaptotagmin Binding to Botulinum Neurotoxins. Biochemistry, 2020, 59, 491-498.	2.5	2
96	The First Structure of an Active Mammalian dCTPase and its Complexes With Substrate Analogs and Products. Journal of Molecular Biology, 2020, 432, 1126-1142.	4.2	2
97	Re-engineering Botox. Science, 2021, 371, 782-782.	12.6	2
98	A nucleotide-sensing oligomerization mechanism that controls NrdR-dependent transcription of ribonucleotide reductases. Nature Communications, 2022, 13, 2700.	12.8	2
99	Inhibition of chlamydial class Ic ribonucleotide reductase by Câ€ŧerminal peptides from protein R2. Journal of Peptide Science, 2011, 17, 756-762.	1.4	1
100	The C repressor of the P2 bacteriophage. Journal of Biomolecular NMR, 2016, 64, 175-180.	2.8	0